



## TRIBOLOGICAL INFLUENCE OF THE CLEARANCE IN THE HIP PROSTHESIS

Tiberiu LAURIAN, Andrei TUDOR

*Polytechnic University of Bucharest, tlaurian@omtr.pub.ro*

### **S u m m a r y**

*The longevity of total hip arthroplasties is significantly reduced by the wear of joint surfaces. Wear is the result of the product between contact pressure and sliding distance that is generated by the patient's daily activity. While the sliding distance can be calculated using the variation of angles describing the hip kinematics, determining the pressure distribution prove to be difficult especially because the Hertz contact hypotheses are not valid in the case of ball-in-socket joints. With the aid of finite element method it was possible to study the behavior of hip joint prostheses having different radial clearances under similar loads. It is emphasized the influence of radial clearance on the contact area, maximum contact pressure and pressure distribution.*

**Keywords:** *hip prosthesis, wear, FEM model, contact pressure, UHMWPE.*

### **1. INTRODUCTION**

The importance of studying the wear behavior of artificial joint prostheses does not need to be emphasized. Since the first successful attempts to replace diseased joints with joint prostheses, many scientists struggled to find ways of prolonging their life. As it is well known, the wear of UHMWPE and the resulting debris are the primary cause of long time implant failure.

As numerous papers show, the clearance between the two articulating surfaces plays an important role in the friction and wear processes taking place in the prosthesis. Of particular interest is the contact pressure distribution on the joint surface, as it indicates the regions of most elevated stress and gives its magnitude.

The finite element method (FEM) has become the method of choice to analyze the mechanical behavior of objects characterized by a complicated shape and which are subjected to complex loading. As such, it is widely used in the study of contact between solids.

### **2. MATERIALS AND METHODS**

The work was divided into three steps. First, a FE model of the cup/head assembly was ran to simulate the behavior under a variable load. The second step was the calculation of the sliding distance for a series of points evenly distributed on the femoral head. Finally, the third step consisted in the calculation of the wear depth for each of the points considered at the second step using the Archard's wear law. After obtaining the wear depth for a fairly large number of points, the total volumetric wear can then be calculated.

FE model of a total hip prosthesis was constructed using a commercial available FEM package (ANSYS 6.1, SAS IP Inc., USA). The FE model consists of a perfectly rigid femoral head articulating into an UHMWPE acetabular cup. In order to investigate the influence of the clearance on the wear of total hip joint prostheses, ten different cases were studied. For all cases the outer and inner diameter of the cup were 60mm and 22mm respectively. Only the clearance between the femoral and acetabular component was different

from one case to another. The ten cases and their corresponding clearances are listed in Table 1.

The acetabular cup was modeled with one of the most accurate 3-D finite element, which is the 20-node brick (hexahedral) element.

Direct generation of brick elements in a hemispherical volume proved to be impossible. One solution to this problem would have been to use tetrahedral or modified hexahedral elements (15 node wedges) at the polar region.

**Table 1**

Case no.	Absolute radial clearance [mm]	Relative clearance
1	0	0 %
2	0.005	0.045 %
3	0.01	0.09 %
4	0.02	0.18 %
5	0.05	0.45 %
6	0.1	0.9 %
7	0.2	1.8 %
8	0.3	2.7 %
9	0.4	3.6 %
10	0.5	4.5 %

The mixing of elements (tetrahedral or wedges and hexahedral) is often the cause of irregular stress concentrations that can greatly affect the results. In this circumstance, the volume of the acetabular cup was divided into five volumes, each with six sides.

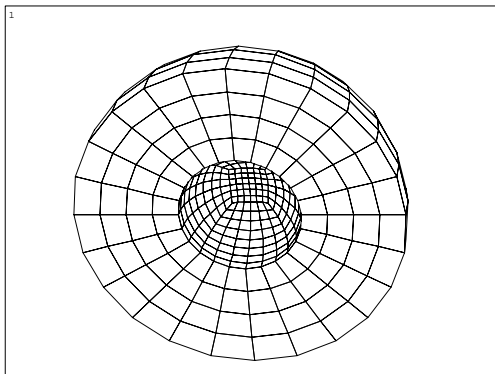


*Figure 1 FEM model of the acetabular cup based on 20-node brick elements.*

This meshing was inspired by the design used in [1,2,3]. The difference consists in the use of higher order elements (20 node) instead of lower order (8 node) hexahedrons as in other designs.

The mesh was formed of 914 hexahedral elements and 228 8-node quadrilateral contact elements (ANSYS CONTA174). The femoral head was represented by a rigid sphere defined as a single element (ANSYS TARGE169).

## 2.1 Material properties

The UHMWPE was considered to have an elasto-plastic behavior. It is assumed that the material deforms linearly elastic until a certain point (yield point). After this point, the material exhibits nonlinear rate-independent plasticity. Classical rate-independent plasticity theory incorporates a flow rule in which the equivalent stress is based on the von Mises yield criterion.

When characterizing the mechanical behavior of UHMWPE at large deformations, it is necessary to adopt a description of the stress-strain curve in terms of true stress and true strain. In Figure 2 is illustrated the nonlinear material behavior of UHMWPE, in terms of true stress and true strain and in Table 2 are listed the main mechanical properties of UHMWPE GUR 4150. The curve was adopted from Kurtz [4].

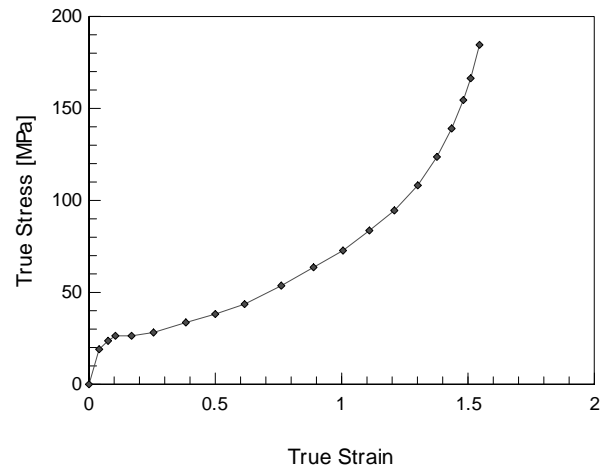


*Figure 2 The true stress vs. true strain behavior of UHMWPE 4150 adopted from [4] (the points represent tabular data input in the FEM program).*

**Table 2**

Mechanical properties for UHMWPE GUR 4150	
Young modulus	600 MPa
Yield stress	19 MPa
Poisson coefficient	0.46

The contact between the two bodies was considered as a contact between a rigid and a deformable body and the sliding between them was assumed to follow the Coulomb's law. The friction coefficient between the two surfaces was taken  $\mu=0.12$ .

## 2.2 Loading

The force components and the acetabular cup orientation were defined relative to a Cartesian coordinate system fixed to the pelvis and having the origin in the cup center of symmetry and the three axes ( $x, y, z$ ) pointing towards anterior, superior and lateral directions, respectively. The acetabular cup was considered to have an inclined position at  $30^\circ$  in the coronal plane ( $yOz$ ) relative to the horizontal plane.

The cup was fixed on its entire outer surface and the rigid femoral ball was pressed against the cup following a pattern that simulates the physiologic conditions. In Figure 3 is shown the load pattern. The load pattern was adopted from Bergmann [5] and simplified in order to obtain a manageable number of load steps necessary for the FEM input file. A number of five load steps were considered and the three forces vary linearly from one load step to the next.

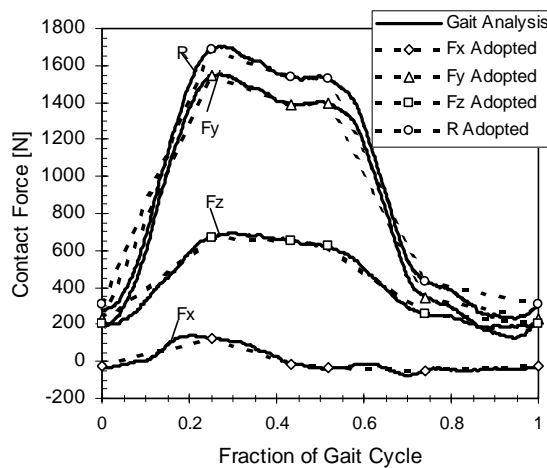


Figure 3 Load variation during the gait cycle.  $F_x$  acts along the walking direction,  $F_y$  on vertical direction and  $F_z$  on medio-lateral direction. Dotted lines represent the simplified force variations.

## 2.3 Calculation of the sliding distance

Sliding distance plays an important role in the wear rate. Developing a wear model that takes into consideration the entire gait cycle and couples the polyethylene contact stresses and sliding distances represents a powerful tool to assess the long time behavior of joint prostheses.

In order to find the corresponding sliding distances for the points situated on the bearing surface of the cup, two coordinate systems, one for the head and one for the cup, were defined with the origins in the rotation center of the prosthesis. One component (femoral head) was maintained fixed

while the other (acetabular cup) rotated around the first following a simplified motion, which approximates the walking motion. The motion waveforms were adapted from Saikko [6] and are shown in Figure 4.

The numerical computations were performed using MATLAB (MathWorks, Inc., Natick, MA, USA). The Euler sequence used in this study was  $FE \rightarrow IER \rightarrow AA$ .

An arbitrary point  $\mathbf{M}$  fixed on the cup surface was rotated from its initial position  $\mathbf{M}_0(x_0, y_0, z_0)$  to consecutive new positions  $\mathbf{M}_1, \mathbf{M}_2, \dots$  until it reached again its initial position  $\mathbf{M}_0$ . The number of discrete positions was 10. The coordinates  $(x_i, y_i, z_i)$  for a point  $\mathbf{M}_i$  on the slide track were obtained by multiplying the vector describing the initial position  $\mathbf{r}_0 = [x_0, y_0, z_0]$  with the three rotation matrices  $R_x, R_y, R_z$ :

$$\mathbf{r}_i = R_x(\alpha_i) \cdot R_y(\beta_i) \cdot R_z(\gamma_i) \cdot \mathbf{r}_0 \quad (1)$$

where:

$$R_x(\alpha) = \begin{bmatrix} \cos \alpha & \sin \alpha & 0 \\ -\sin \alpha & \cos \alpha & 0 \\ 0 & 0 & 1 \end{bmatrix}$$

$$R_y(\beta) = \begin{bmatrix} \cos \beta & 0 & -\sin \beta \\ 0 & 1 & 0 \\ \sin \beta & 0 & \cos \beta \end{bmatrix}$$

$$R_z(\gamma) = \begin{bmatrix} 1 & 0 & 0 \\ 0 & \cos \gamma & \sin \gamma \\ 0 & -\sin \gamma & \cos \gamma \end{bmatrix}$$

The angles  $\alpha, \beta, \gamma$  represent the waveforms of  $FE, AA$  and  $IER$  respectively.

The points  $\mathbf{M}_i$ , for which the corresponding sliding distances were calculated, were the centers of the contact elements lined on the cup bearing surface.

## 2.4 Wear Calculation

For wear calculation, the Archard's equation was considered as in [1,3,7]. The amount of wear removed from the UHMWPE cup is assessed by the equation:

$$V = K \cdot \frac{l}{H} \cdot p_N \cdot S \quad (2)$$

where:  $V$  is the linear wear volume,  $H$  is the hardness of the material,  $p_N$  is the normal contact force and  $K$  is a proportionality constant. The wear volume correlates with material properties, load and motion. Because the load and motion are variable throughout the joint surface, Archard's wear law must be modified into an incremental form. So, the equation (2) becomes:

$$dV = \frac{K}{H} \cdot \frac{\sigma_N}{dA} \cdot dS \quad (3)$$

where  $\sigma_N$  is the normal contact stress,  $dA$  is the infinitesimal contact area and  $dS$  the infinitesimal sliding distance.

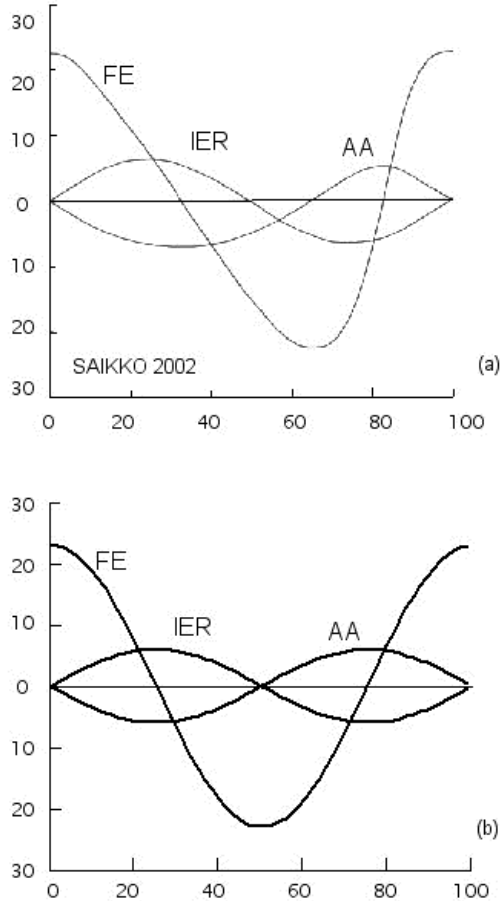


Figure 4 Gait waveforms from Saikko [6] (a) and adopted for this study (b); FE=flexion-extension, AA=abduction-adduction; IER=internal external rotation

Eliminating the infinitesimal contact area from the equation (3) and replacing  $K/H$  with  $k_w$ , we get:

$$dh = k_w \cdot \sigma_N \cdot dS \quad (4)$$

where  $dh$  is the infinitesimal wear depth and  $k_w$  is the wear coefficient (in units of  $mm^3/(Nm)$ ).

To get the wear depth at a certain point after one cycle of motion, we must integrate equation (4) over the sliding distance at that point:

$$h_i = \int_{S_i} k_w \cdot \sigma_{Ni} \cdot dS \quad (5)$$

Integrating again over the entire surface of the cup, the total wear volume per cycle of motion can be calculated:

$$V = \int_{A_{tot}} \left( \int_S k_w \cdot \sigma_N \cdot dS \right) dA \quad (6)$$

The most difficult to obtain is the parameter  $k_w$  (wear coefficient). It can be obtained experimentally on wear testers such as pin-on-disk or other configurations. Papers concerned with the wear in total hip prostheses reported values in the range  $0.8 \div 2 \cdot 10^{-9} mm^3/N \cdot mm$  [3,7-9]. For this study it was adopted a wear coefficient  $k_w = 1.0656 \cdot 10^{-9} mm^3/N \cdot mm$  as in [7].

### 3. RESULTS

In Figure 5 is shown the distribution of contact pressure for case no. 1. The maximum is located at a certain angle relative to the pole and varies in the range  $10.9 \div 11.7 MPa$ , increasing with the increase of clearance.

At the first look one can say that from the point of view of maximum contact pressure, the smaller the clearance, the smaller the contact pressure and hence, the smaller the wear of the acetabular cup. This is true only until a certain clearance below which the maximum pressure migrates towards the rim of the cup and increases exponentially with the decrease of clearance. This means that both extremes (very small or very large clearance) lead to dangerously high values of the contact pressure.

After FE simulations were performed for the ten cases, the contact pressure distributions were introduced as input data in a computer code which integrated them in equation (6). The results are listed in Table 3 and plotted in Figure 9.

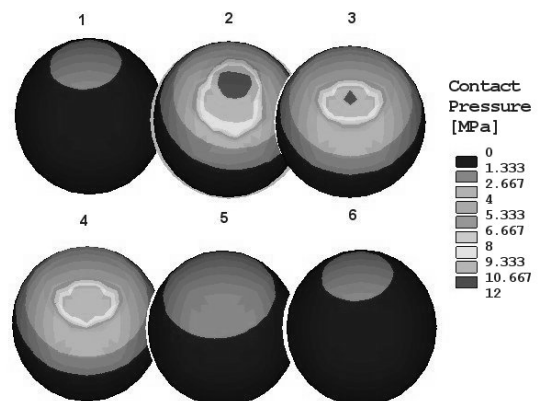


Figure 5 Evolution of the contact pressure distribution on the acetabular cup surface during a gait cycle.

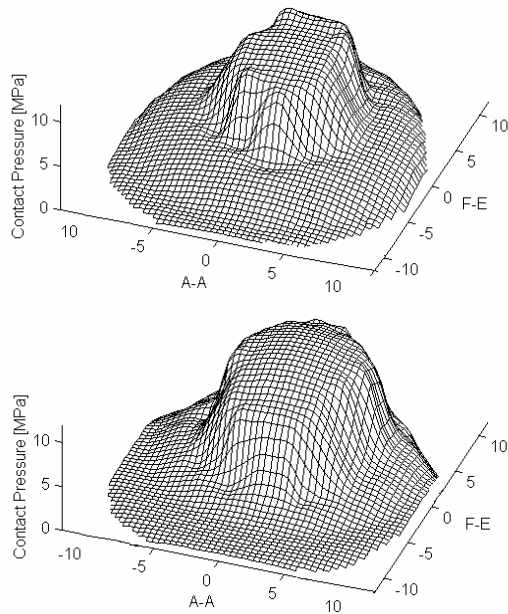


Figure 6 Pressure distribution plotted over the projected contact area for 0.01mm clearance (up) and for 0.5mm clearance (down).

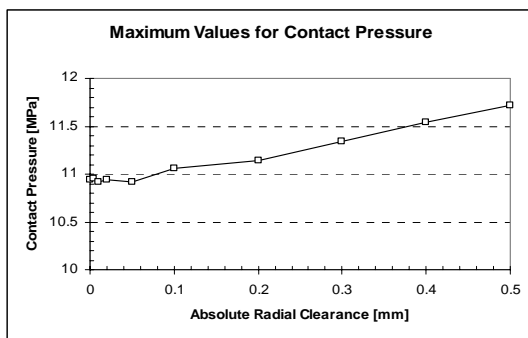


Figure 7 Variation of the maximum contact pressure with radial clearance.

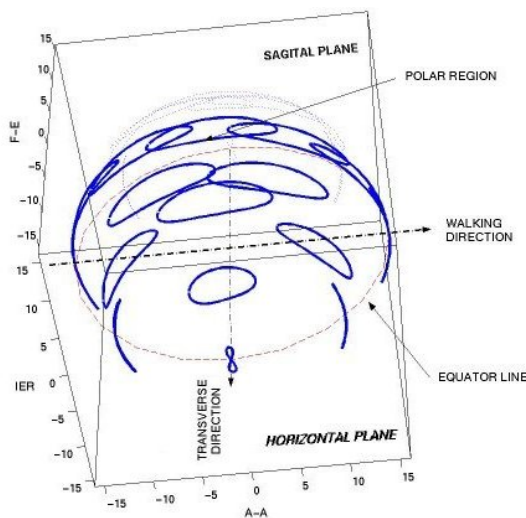


Figure 8 Slide tracks for several points on the bearing surface of the cup.

The slide tracks resulted from the simplified waveforms were similar with the slide tracks obtained by Saikko and Calonius [6,10]. Figure 8 shows the slide tracks for several points distributed on the femoral head surface. The tracks were mainly ovals except for the equatorial regions where “eight” shaped or straight tracks were obtained.

Table 3

Case no.	Relative clearance [%]	Wear volume after 10 <sup>6</sup> cycles [mm <sup>3</sup> ]
1	0 %	20.62
2	0.045 %	20.59
3	0.09 %	20.53
4	0.18 %	20.477
5	0.45 %	20.26
6	0.9 %	19.96
7	1.8 %	19.47
8	2.7 %	18.99
9	3.6 %	18.65
10	4.5 %	18.36

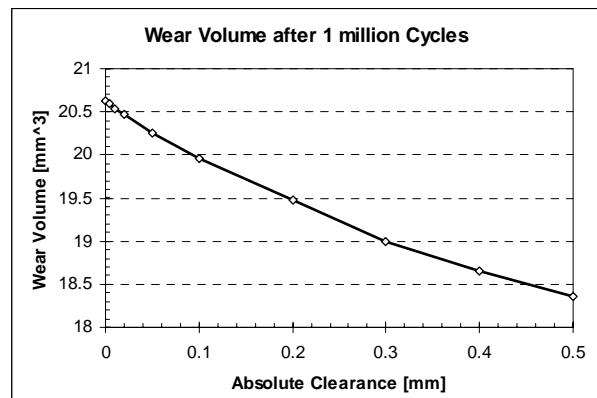


Figure 9 Variation of wear volume with the radial clearance.

#### 4. DISCUSSION

The obtained wear rates are similar with those reported by other authors (Table 4). It can be seen that the increasing of prosthesis clearance induces a slight decrease of the wear rate (Fig. 9). As the clearance between the two bearing surfaces becomes larger, the effective contact area decreases (e.g. the contact is not established over the entire cup inner surface). In the same time, the load is distributed over a smaller area and naturally, the maximum pressure is higher. The pressure rising should lead to an increase of the wear rate but, the wear rate is also proportional to the contact area and therefore the wear rate is not influenced by this variation of the contact pressure and contact area. It is the sliding distance that plays the important role in the wear rate because it is not the same for every

point on the bearing surface. In this case, the distribution of the sliding distances is the factor that determines if the wear rate increases or decreases with the clearance.

Even if the wear rate would be lower, the large clearances are not desirable because the penetration is higher and the maximum equivalent stress is also higher. So, the risk of plastic deformations and "boring" of the head into the cup is very high for large clearances. With the increase of the clearance, a "pocket" of maximum equivalent stress nucleates in the substrate. This may lead to delamination (often met at knee prostheses) which can greatly shorten the prosthesis life.

The obtained wear rates may be lower in comparison with many retrieval studies. One reason

may be the relative lower loading forces used in the present work (peak load 1700N). Also, the present study did not take into account the creep of polyethylene. Many clinical wear data incorporates also the creep without separating it from the real wear volume. Teoh [1] reported an increase of wear when the clearance was too big or too small. He found an optimum around 0.1 mm clearance for the 32 mm prosthesis.

Unlike the reported results of Teoh, in this study an optimum clearance may be stated only if considering additional factors beside the wear volume such as the penetration of the head into the cup and the maximum equivalent stress.

**Table 4**

Author	Method	Materials	Wear rate [mm <sup>3</sup> /10 <sup>6</sup> cycles]	Wear coefficient [mm <sup>3</sup> /N·m]	Head diam. [mm]
V. Saikko [11]	Hip simulator	CoCrMo/PE	1.4÷61	$2.7 \times 10^{-8} \div 1.2 \times 10^{-6}$	32
S.H. Teoh [1]	FE model	metal/PE	53.68÷122.27	$1.066 \times 10^{-6}$	32
Maxian [7]	FE model	metal/PE	13	$10.656 \times 10^{-7}$	22
			16		28
			18		32
			42		32
J.S. Wu [3]	FE model	metal/PE	52	$0.8 \times 10^{-6}$	22
			58.4		28
			58.4		32
K. Brummit [12]	Hip simulator	stainless steel/PE	8÷25	-	22.25
J. Lancaster [13]	Pin-on-plate	different mat./PE	-	$6.1 \div 16.5 (\times 10^{-9})$	-
I.C. Clarke [14]	Hip simulator	alumina/PE	23.2	-	22.25
			31.9		26
			32.8		28

## REFERENCES

- [1] S. Teoh, W. Chan, R. Thampuran, An elasto-plastic finite element model for polyethylene wear in total hip arthroplasty, *J. Biomechanics*, 35(2002) 323-330.
- [2] S. M. Kurtz, et al., Backside nonconformity and locking restraints affect liner/shell load transfer mechanisms and relative motion in modular acetabular components for total hip replacement, *J. Biomechanics*, 31 (1998) 431-437.
- [3] J. Wu, J-P. Hung, et. al., The computer simulation of wear behavior appearing in total hip prosthesis, *Comp. Methods and Progr. In Biomedicine*, 2002.
- [4] S. M. Kurtz, et al., The yielding, plastic flow, and fracture behavior of ultra-high molecular weight polyethylene used in total joint replacements, *Biomaterials*, 19 (1998) 1989-2003.
- [5] G. Bergmann, G. Deuretzbacher, M. Heller, F. Graichen, A. Rohlmann, J. Strauss, G.N. Duda, Hip contact forces and gait patterns from routine activities, *J. Biomechanics*, 2001 (34) 859-871.
- [6] V. Saikko, O. Calonijs, Slide track analysis of the relative motion between femoral head and acetabular cup in walking and in hip simulators, *J. Biomechanics*, 35(2002) 455-464.
- [7] T. Maxian, T. Brown, D. Pedersen, J. Callaghan, A sliding-distance-coupled finite element formulation for polyethylene wear in total hip arthroplasty, *J. Biomechanics*, Vol. 29, (1996) 687-692.
- [8] V. Saikko, T. Ahlroos, O. Calonijs, J. Keranen, Wear simulation of total hip prostheses with polyethylene against CoCr,

- alumina and diamond-like carbon, *Bio-materials* 22 (2001) 1507-1514.
- [9] V. Saikko, A multidirectional motion pin-on-disk wear test method for prosthetic joint materials, *J. Biomed. Mater. Res.* 41-1 (1998) 58-64.
- [10] O. Calonius, V. Saikko, Slide track analysis of eight contemporary hip simulator designs, *J. Biomechanics*, 35 (2002) 1439-1450.
- [11] V. Saikko, A three-axis hip joint simulator for wear and friction studies on total hip prostheses, *Advances in medical tribology*, Edited by D. Dowson, *Mech. Eng. Publ.*, 1998, 35-45.
- [12] K. Brumitt, C.S. Hardaker, Estimation of wear in total hip replacement using a ten station hip simulator, *Advances in medical tribology*, Edited by D. Dowson, *Mech. Eng. Publ.*, 1998, 47-50.
- [13] J.G. Lancaster, D. Dowson, G.H. Isaac, J. Fisher, The wear of ultra-high molecular weight polyethylene sliding on metallic and ceramic counterfaces representative of current femoral surfaces in joint replacement, *Advances in medical tribology*, Edited by D. Dowson, *Mech. Eng. Publ.*, 1998, 109-116.
- [14] I.C. Clarke, V. Good, L. Anissian, A. Gustafson, Charnley wear model for validation of hip simulators-ball diameter versus polytetrafluorethylene and polyethylene wear, *Advances in medical tribology*, Edited by D. Dowson, *Mech. Eng. Publ.*, 1998, 117-128.